# Enhanced Pool Boiling Heat Transfer on Copper Foam Welded Surfaces

*HU Zhuoyang, CUI Enhua, KHAN Muhammad Niaz, ZHANG Qian, CHEN Xuefeng, JI Keju**

College of Mechanical and Electrical Engineering, Nanjing University of Aeronautics and Astronautics, Nanjing 210016, P.R. China

(Received 15 April 2022; revised 9 May 2022; accepted 28 June 2022)

**Abstract:** Enhanced pool boiling heat transfer of the porous structure is critical to the thermal management technology. In this paper, pool boiling heat transfer experiments are performed on copper foam welded surfaces in de-ionized water to investigate the effects of basic parameters of copper foam on heat transfer enhancement. Boiling phenomenon is observed to facilitate the understanding of enhancement mechanism. The results show that copper foam welded surfaces can significantly enhance the pool boiling heat transfer performance, reduce the boiling incipience temperature by 7—9 ℃, and reach two times heat transfer coefficient compared with smooth plain surfaces due to numerous nucleation sites, extended surface areas, and enhanced turbulent effect. Pore density and thickness of foam have two side effects on heat transfer.

**Key words:** copper foam; porous surface; enhanced heat transfer; pool boiling

**CLC number:** TB61+1 **Document code:** A **Article ID:** 1005-1120(2022)S-0032-10

## 0 Introduction

With the rapid development of advanced technologies such as aerospace and high-end electronic equipment, heat dissipation of electronic devices and components is being a key obstacle, and conventional cooling methods no longer meet the demand of high-heat-flux removal, leading to challenge of discovering high-efficient cooling technologies[1]. Pool boiling heat transfer, as a phase change cooling technique with high heat transfer efficiency by utilization of the latent heat, has become a burgeoning area of research. Some advanced techniques evolved from it such as heat pipe and vapor chamber have great potential to be applied to solve these problems. In addition, the enhancement of pool boiling heat transfer can increase energy efficiency of boilers in power plants, evaporators in refrigeration system and other industrial equipments[2]. Therefore, the research on how to enhance boiling heat transfer is of great significance.

As is known, boiling surface topography has great influence on boiling performance, so many researchers focus on enhanced pool boiling heat transfer by modifying surface topography or creating novel surfaces through various approaches classified as physical methods, chemical methods, and electrochemical methods. Physical methods include mechanical workout[3-5], sintering[6], welding, spraying[7], deposition[8], direct attached[9-10], etc. Chemical methods include erosion or etching[11], chemical vapor deposition (CVD)[12-13], etc. Electrochemical methods include electroplating[14-17], anodizing[18-19], etc. Using these methods different surface structures such as microchannel, microfin, microporous layer, oriented porous array and their composite structure are fabricated for these structures have one or more advantages of extending surface area, increasing nucleation site, and providing capillary suction and separated path for vapor-liquid motion[9]. Among the

*Corresponding author, E-mail address: jikeju@nuaa.edu.cn.

**How to cite this article**: HU Zhuoyang, CUI Enhua, KHAN Muhammad Niaz, et al. Enhanced pool boiling heat transfer on copper foam welded surfaces[J]. Transactions of Nanjing University of Aeronautics and Astronautics, 2022, 39(S): 32-41.
http://dx.doi.org/10.16356/j.1005-1120.2022.S.005

many structures that enhance boiling heat transfer, porous structures, especially cross-scale porous structures with high thermal conductivity, have important applications in the field of fluid-solid interface heat transfer.

The open-celled metal foam fabricated by electrodeposition method is a novel kind of porous metal structure with high thermal conductivity, high porosity, large specific surface area and light weight, being suitable for heat transfer applications[20]. However, the existing literatures mostly focus on convective heat transfer or single-phase heat transfer, and fewer studies report boiling heat transfer enhancement with metal foam structure, among which the general agreement is not reached yet. The purpose of this paper is to experimentally investigate the effects of basic parameters on pool boiling heat transfer with copper foam covered surface, and to discuss the detailed enhancement mechanism to provide a more comprehensive engineering design reference database for metal foam being used as thermal management materials.

# 1 Experiment

## 1.1 Experimental apparatus

A schematic diagram of experimental setup is shown in Fig.1. It mainly consists of four parts: the heating section, the boiling chamber, the condensation section, and the data acquisition system. The

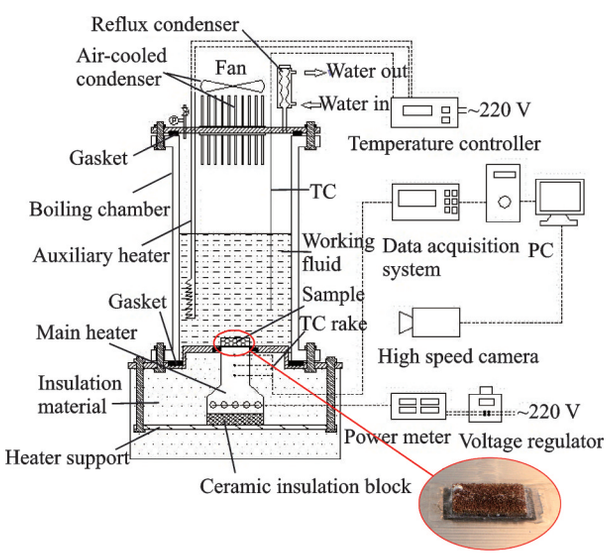


Fig.1 Schematic of experimental setup

heating section includes a machined copper block with five cartridge heaters inserted into the square groove of bottom part. Each cartridge heater can provide the maximum thermal power of 200 W, and total maximum power is 1 000 W. The power meter is used to monitor the power of heat generated.

The boiling chamber is a 10 cm×10 cm×25 cm container made of transparent glass with 6 mm thickness at the four sides, a copper plate at the top, and a stainless-steel plate at the bottom. Rubber gaskets are used for sealing between them. The transparent boiling chamber is designed for visualization of boiling phenomenon. A high-speed camera is used to record the bubble formation. At the center of the bottom plate, a rectangular hole is drilled to fit the heating block. The gap between them is filled with teflon and epoxy glue for sealing and insulation. Additionally, silicone rubber glue is used to prevent the formation of micro-cracks at the edges that would cause bubble nucleation disturbing the experimental result.

Condensation section is at the top of the boiling chamber. The provided heat dissipation is up to 1 200 W. The heat sink is attached on its both sides to increase the cooling area, and a fan is connected with an adjustable power supply to condense the vapor induced during the boiling of working fluid. The emptying method with water is used to achieve a container vacuum and remove non-condensing gases. The pressure in the vessel is obtained by measuring the water temperature checklist. The data acquisition system includes power meter, PC, temperature controller, data acquisition, high speed camera, SEM and more.

An auxiliary heater is fixed in the chamber and connected with a temperature controller to keep the working fluid saturation condition during the experiment.

## 1.2 Test sample and working fluid

Fig.2 shows photos of copper foams with three kinds of pore density (Pores per inch, PPI) used in this study (shown in Figs.2(a), 2(b) and 2(c)). The copper foam is prepared in our laboratory by first subjecting polyurethane foam to conductive

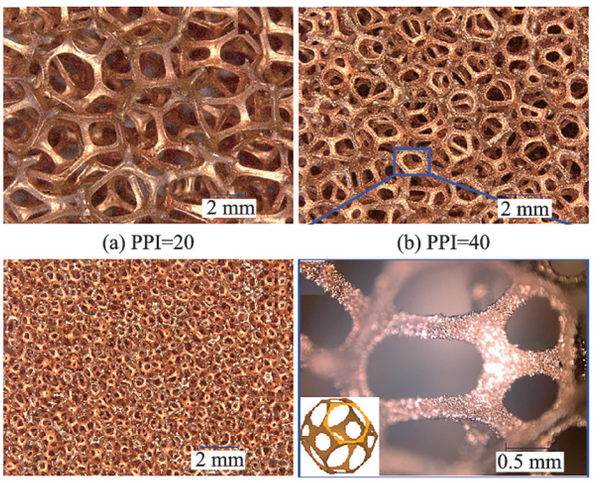


Fig.2 Optical images of cooper foam with different PPI

treatment (conductive graphite colloid coating), and then carrying out a copper electroplating process and heat treatment. This 3-D connected metal skeleton structure with tetrakaidecahedron-like open cells has many idiosyncratic properties such as high thermal conductivity, high porosity, large specific surface area and light weight, thus being highly appropriate for heat transfer application. It is noting from SEM images that the ligament surface is rough formed by copper particle deposition and filled with numerous micro-pores generated during heat treatment process (shown in Fig.3), which may contribute to potential nucleation sites. The structural parameters of copper foam with different pore densities are shown in Table 1.Since the effective thermal conductivity of high porosity metal foams is related to the porosity[20-21], and specific surface area depends mainly on the porosity and the pore diameter[22], the PPI and thickness are used to analyze the effects of copper foam structure on boiling heat transfer due to approximately the same porosity of the tested foams. The thickness of copper foams is selected following the principle of one unit cell at least and five at most for the sake of representation. Deionized water is used as the working fluids in the experiments.

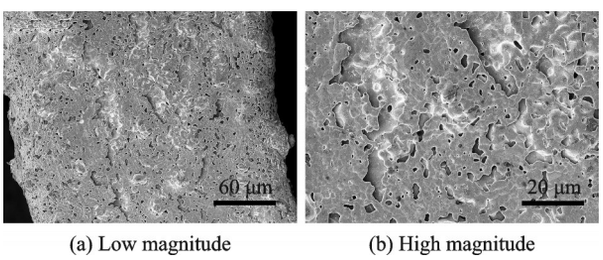


Fig.3 SEM images of foam metal skeleton surface

**Table 1 Characteristic parameters of copper foams used in the paper**

| PPI | Porosity $\varepsilon$/% | Average aperture $d_p$/mm | Density $\rho$/(g·cm$^{-3}$) | Thickness $\delta$/mm |
|---|---|---|---|---|
| 20 | 94.3 | 3.2 | 0.16 | 4, 8, 12, 15 |
| 40 | 94.0 | 1.8 | 0.23 | 2, 4, 6, 8 |
| 80 | 93.8 | 0.9 | 0.49 | 1, 2, 3, 4 |

### 1.3 Experimental procedures

The experimental procedures mainly involve welding the sample with the copper block, charging working fluid into the boiling chamber, and conducting formal boiling experiment.

In order to ensure small thermal resistance, the copper foam is directly welded on the copper block with tin. Firstly, the top surface of the copper block is cleaned by methanol and baked in an oven. Then it is taken out and heated by the cartridge heaters until its temperature reaches the melting temperature of the tin at the top copper surface, leaving a thin tin film. At last, turn off the cartridge heaters and cool down the copper block with high pressure nitrogen gun quickly to prevent the sample from oxidation under high temperature. After that, the test sample is cleaned again. In this mean the copper foam is welded tightly with the copper block, and the thickness of tin is about 0.1 mm, much less than the thickness of test sample, thus the contact thermal resistance is considerably eliminated.

After welding and well assembled, the working liquid is charged in the boiling chamber. The top liquid level is kept higher than the test surface by about 120 mm. The main heater and auxiliary heater are both turned on to keep boiling for 1 h to remove the non-condensable gas in the foam and liquid.

Afterward, the liquid is naturally cooled and the system is ready for formal boiling experiment. We start an experiment from a small heat flux density of 1—2 W/(cm$^2$·K) on the test surface, and about 3—4 min later, the temperature of each thermocouple reaches nearly stable. If the variation of copper block temperature is within 0.5 ℃ in approximate 10 min, the heat flux density is increased by a

step of 5—8 W/(cm²·K). The procedure is repeated until reaching critical heat flux density (CHF) or the heater limit.

### 1.4 Data analysis

The other sides of the copper block is wrapped by well thermally insulating material (aluminum silicate fiber with coefficient of thermal conductivity $\lambda<0.03$ W/(m·K)) only leaving the top surface immersed in water. And the thermal conductivity of oxygen-copper is high. A one-dimensional steady-state heat conduction in the upper part of the heater is assumed. Such assumption can also be found in Ref.[14]. Hence, the approximate linear temperature distribution can be plotted by the tested temperatures $T_1$, $T_2$ and $T_3$. According to Fourier's law, the heat flux density can be expressed as

$$q=-k_s\left.\frac{\mathrm{d}T}{\mathrm{d}z}\right|_w \tag{1}$$

where $k_s$ is the copper thermal conductivity, $\left.\frac{\mathrm{d}T}{\mathrm{d}z}\right|_w$ the temperature gradient at the heater top surface, and $z$ the coordinate perpendicular to the substrate surface. The relationship between $T$ and $z$ can be described as $T=a_1+a_2z$ by using least square method, where $a_1$ and $a_2$ are correlated constants based on the three measured temperatures on the copper block.

The surface superheat $\Delta T_{sat}$ is defined as the surface temperature of $T_w$ minus $T_{sat}$, where $T_w$ is the temperature at the base surface, and $T_{sat}$ the saturation temperature of water at atmospheric pressure, regarded as 100 ℃ in the present study. Heat transfer coefficient is calculated as

$$h=\frac{q}{T_w-T_{sat}} \tag{2}$$

Thus, the uncertainty $h$ can be calculated by

$$\Delta h=\sqrt{\left(\frac{\partial h}{\partial q}\right)^2(\Delta q)^2+\left(\frac{\partial h}{\partial T_w}\right)^2(\Delta T_w)^2+\left(\frac{\partial h}{\partial T_{sat}}\right)^2(\Delta T_{sat})^2} \tag{3}$$

By substituting Eq.(2) into Eq.(3), the relative uncertainty $h$ can be calculated as

$$\frac{\Delta h}{h}=\sqrt{\left(\frac{\Delta q}{q}\right)^2+\left(\frac{\Delta T_w}{T_w-T_{sat}}\right)^2+\left(\frac{\Delta T_{sat}}{T_w-T_{sat}}\right)^2} \tag{4}$$

All the temperatures measured using T-type thermocouples in this study have the maximum uncertainties of 0.1 ℃, and the relative uncertainty of heat flux density $\Delta q/q$ is estimated to be smaller than 6.5% according to the same method in references. The maximum relative uncertainty of heat transfer coefficient is obtained at the condition of the smallest test surface temperature and calculated to be 10.4%.

## 2 Results and Discussion

### 2.1 Visualization of boiling phenomenon

Fig.4 shows boiling curves of the copper foam

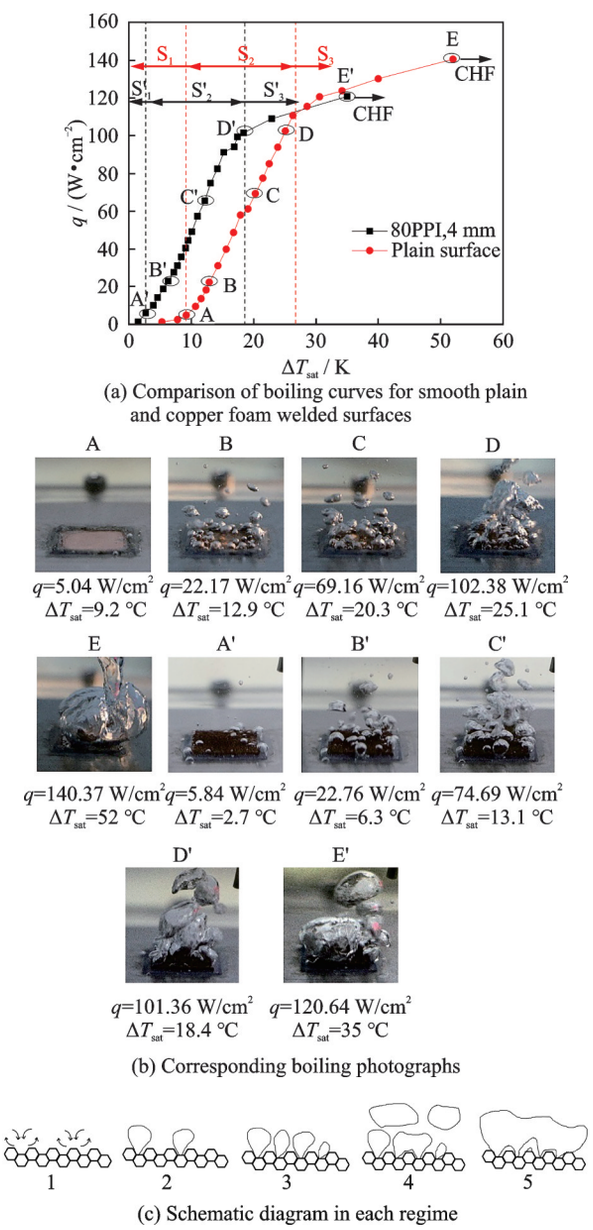


(a) Comparison of boiling curves for smooth plain and copper foam welded surfaces

(b) Corresponding boiling photographs

(c) Schematic diagram in each regime

Fig.4 Pool boiling characteristics and bubble formation characteristics of copper foam

with pore density of 80 PPI and thickness of 4 mm and plain surface as well as the bubble formation of each stage. Before boiling incipience, the heat flux density is low and the wall superheat is slight, which is insufficient to provide the energy required for bubble nucleation growth. This stage mainly depends on outward expansion of local overheated liquid to form the natural convection for heat exchange, which provides low heat transfer efficiency. With the increase of heat flux density, the wall temperature rises and gradually reaches the boiling incipience temperature. Bubble nucleation takes place at some specific positions, and the bubbles gradually grow by absorbing energy of the surrounding overheated liquid. With increasing heat flux density further, more nucleation sites are activated, and more bubbles are generated and remained in independent scattered forms. This stage presents a large number of bubbles with high emission frequency and high rising velocity, during which the interference between bubbles is slight and the resistance to vapor release is not obvious, resulting in higher heat transfer efficiency. The heat flux density increases continuously, single bubble grows and adjacent bubbles begin to coalesce into a bigger one, leading to the metallic skeleton more resistant to bubbles rising inside the foam structure to departure, thus the heat transfer efficiency becomes slower. With further increase of the heat flux density, the range of bubbles coalescence expands so wide that a large area of vapor film eventually forms, covering the heated surface and hindering the liquid from flowing towards the heated wall. In this case, a small heat flux density increase would cause a dramatic increase of the wall temperature until the heat flux density limit is reached, which is CHF.

It can be known from A′ in Fig.4(b) that the bubble formation can take place on metal foam welded surface at low heat flux density, decreasing the wall superheat. While the plain surface remains the natural convection state at the similar heat flux density, it shows that the unique structure of metal foam can effectively reduce the temperature of boiling incipience, meaning that the working liquid enters the boiling state at an earlier time. With the increase of heat flux density, the boiling curve of metal foam corresponding to that of smooth plain surface shifts towards the direction of lower wall superheat, showing better heat transfer performance (shown as B′—D′ compared with B—D in Fig.4 (b)). This is contributed to combined effects of large extended surface area of metal foam, numerous nucleation sites on metallic skeletons and capillary-assist liquid suction resulted from evenly-distributed pores. At that moment, the foamed metallic skeletons generate an extraordinary resistance to the bubble release and give rise to the formation of a large area of vapor film, then the liquid reflux is hindered, and the wall temperature increases rapidly until the heat transfer limit is reached. It can be seen that the CHF of foamed metal surface is lower than that of the smooth plain surface (points E and E′), which indicates the heat transfer is weakened by the foamed metal.

In a word, compared with a smooth plain surface, the metal foam welded surface filled with numerous nucleation sites can initiate the working liquid boiling at a lower wall superheat, and the metal foam has an extremely large surface area which expands phase-change heat transfer area when boiling takes place on the pore wall in the metal foam and part of the heating surface. When bubbles grow and rise rapidly within the limited space in metal foam, they produce great impact on and disturbance to thermal boundary layer in the pore, decreasing the thickness of liquid film in the micro-pore, consequently reducing the heat transfer resistance and enhancing the liquid evaporation and heat convection. In addition, the liquid is continuously sucked into the micro-pore under the effect of capillary force, providing sufficient liquid supply, which is also an important reason for heat transfer enhancement. Meanwhile, it should also be noted that irregular skeleton and small pore diameter of the metal foam play a resistant role in bubble release, indicating weakened heat transfer side. Therefore, it is necessary to study the effects of structural parameters of the metal foam on the boiling heat transfer performance from strengthening and weakening aspects.

### 2.2 Pore destiny effect

The pore size directly affects the bubbles release and liquid supplement during boiling, while the pore diameter is closely related to pore density of the metal foam. Thus, it is believed that PPI is critical to boiling heat transfer. As shown in Fig.5(a), compared with the smooth plain surface, the wall superheat $\Delta T_{sat}$ of the copper foam welded surfaces at boiling incipience is 3—5 ℃, 7—9 ℃ lower than that of smooth plain surface, showing the advantage of the metal foam in enhancing the nucleate boiling startability. At low heat flux density (when $q<$ 85 W/cm$^2$ in this experiment), the wall superheat decreases along with the increase of pore density. Among three kinds of pore density tested, the wall superheat of 80 PPI is the smallest. When $q$ is relatively higher, with the increase of $q$, the boiling curves of metal foam tend to be similar to that of smooth plain surface, showing the weakened heat transfer enhancement. Especially for the copper foam welded surface of 80 PPI, when the heat flux density is higher than 100 W/cm$^2$, the heat transfer performance becomes weakened sharply, even lower than the smooth plain surface, finally the CHF is lower than that of smooth plain surface. In this experiment, the specimens of 20 PPI and 40 PPI have not reached CHF, but its value can be predicted from the figure to be higher than that of smooth plain surface. Fig.5(b) shows effect of PPI on heat transfer coefficient. It can be seen that the copper foam welded surfaces with three pore densities all enhance the heat transfer coefficient to some extent. The enhancement ratio is related to pore density and the heat flux density input. The specimen of 80 PPI reaches the maximum (5.9 W/(cm$^2$·K)) at $q$=91 W/cm$^2$ under the experimental thickness of 4 mm, about two times of that of the smooth plain surface.

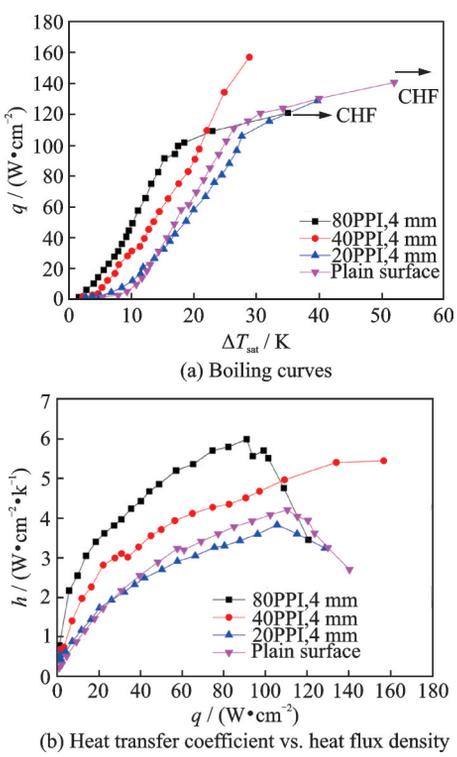


Fig.5 Effect of PPI on boiling curves and heat transfer coefficient under the saturation pool liquid conditions ($\varepsilon \approx 94.0\%$, $\delta$ = 4 mm, $T_{bulk}$=100 ℃)

The observation of bubbles behavior in the boiling process reveals that the bubbles release in some particular places selectively at low $q$. The foam cell diameter $d_p$ restricts the bubble release. On one hand, the higher PPI is, the smaller $d_p$ would be, and the resistance to bubble release would be greater, which deteriorates heat transfer performance. On the other hand, under the condition of the similar porosity, the higher PPI is, the denser the metal skeleton distribution would be. There would be more potential nucleation sites, and the heat transfer area would be larger. Meanwhile, during the boiling process, the bubbles gradually grow and detach. After the bubbles detach from surface, the pressure in the pore of metal foam would temporarily drop. The surrounding fresh liquid is sucked into the metal foam by capillary force for re-evaporation, reaching a stable cycle of liquid-vapor two-phase flow and heat and mass transfer. The smaller the foam pore diameter is, the more significant the capillary force would be, and the more beneficial it would be to the liquid supply during the boiling heat transfer. In consequence, the PPI effect of pool boiling heat transfer enhancement on metal foam welded surface is the result of combined effect of resistance to bubble release, extended surface area, increased potential nucleation sites and liquid supply by capillary force, each of which plays a dominant role in different stages. At low heat flux density regime, the amount of bubbles is not abundant and their form is independent and scattered. The resis-

tance to bubble release is not obvious. The nucleation site density and liquid supply and other intensifying factors dominate. As a consequence, the higher PPI is, the better the heat transfer performance will be. At high heat flux density regime, the boiling is violent. Numerous bubbles generate, mutually coalesce and become larger in volume. The metal skeleton resistances to bubble release become obvious, which gradually develop to a dominant factor. The bubbles generated in the bottom continuously rise to accumulate, coalesce and expand, finally develop into an entire vapor film, impeding fresh liquid sucking into the foam inside. As a result, the temperature of heated wall rises sharply, and the heat transfer enhancement degrades till the CHF is reached.

## 3 Thickness Effect

The thickness of metal foam is also a key factor that affects boiling heat transfer performance. On one hand, the larger the thickness is, the more the metal skeleton is. And the larger the heat transfer area and the more the potential bubble nucleation sites will be, both of which enhance heat transfer. On the other hand, a thicker foam generates larger resistance to bubble release due to longer vapor transport distance, even leading the bubbles to be trapped in the foam structure, which deteriorates the heat transfer. The two opposite effects respectively play a leading role at different stages and the final effect is the result of their competition.

Fig. 6 shows effects of the copper foam thickness with pore density of 20, 40, 80 PPI on the heat transfer performance, where $T_{bulk}$=100 ℃. It can be seen that the heat transfer performance of the metal foam specimens with various parameters, except the specimen of 20 PPI with the thickness of 4 mm, is all improved compared with that of smooth plain surface. And the changing trends stay substantially the same, that is, with the increase of heat flux density, the heat transfer coefficient firstly increases dramatically, and then slows down, finally drops. For specimen with high pore density (e.g., 80 PPI, 4 mm thickness), some local data is even lower than that of the smooth surface. As to the specimen of 20 PPI with the thickness of 4 mm, poor heat transfer performance may result from the dominant role of resistance to bubble release when

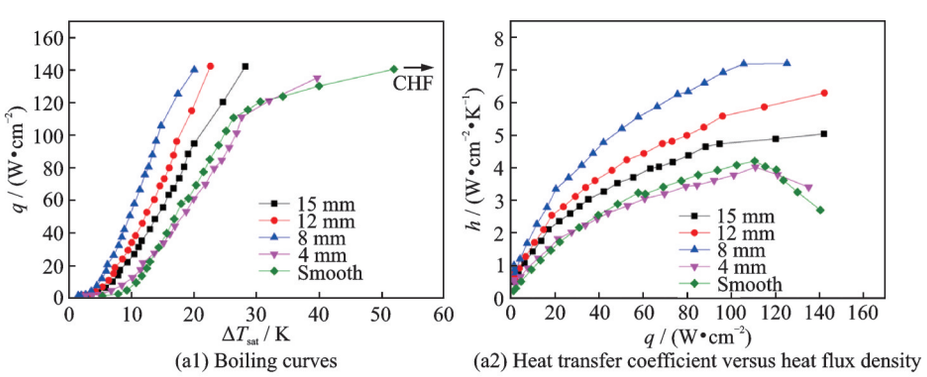


(a1) Boiling curves (a2) Heat transfer coefficient versus heat flux density

(a) PPI=20, $\varepsilon$=94.3%

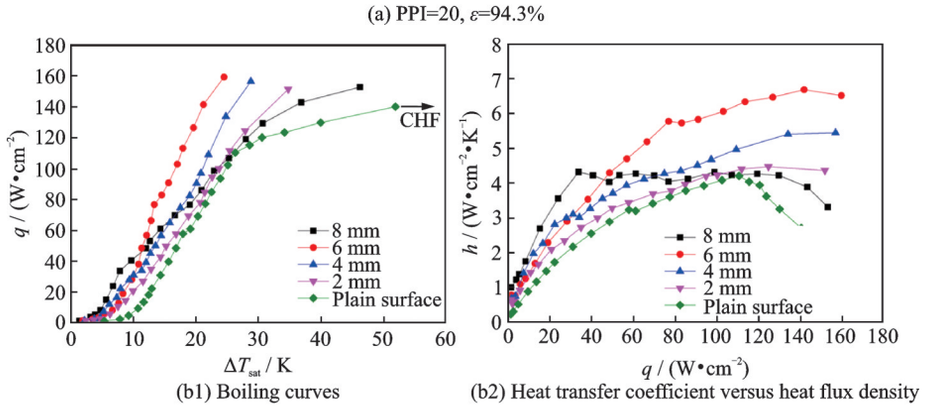


(b1) Boiling curves (b2) Heat transfer coefficient versus heat flux density

(b) PPI=40, $\varepsilon$=94%

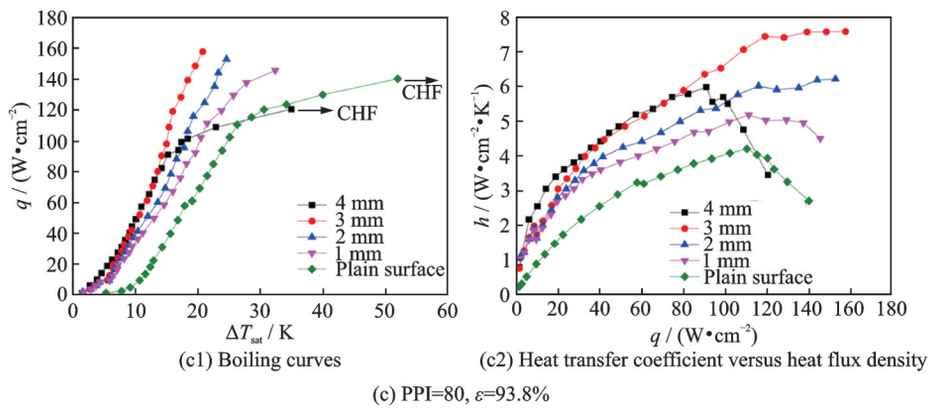


(c1) Boiling curves (c2) Heat transfer coefficient versus heat flux density

(c) PPI=80, $\varepsilon$=93.8%

Fig.6 Effect of copper foam thickness on boiling curves and heat transfer coefficient under the saturation pool liquid conditions

there is insufficient increased nucleation sites and extended surface area due to small thickness and low pore density.

Given a specific PPI value, in low heat flux density regime, bubbles are not enough to coalesce, and the resistance to bubble release is slight, thus the number of bubbles plays a leading role. Larger thickness provides more potential bubble nucleation sites and larger heat transfer area, which can lower the boiling incipience temperature and improve the heat transfer coefficient. With the increase of heat flux density, more bubbles are produced. The bubbles mutually combine and become larger and the resistance of metal skeleton to bubble release becomes dominant, deteriorating heat transfer. Therefore, the specimen with larger thickness presents lower heat transfer coefficient than that of specimen with smaller thickness, and can easily reach CHF. Therefore, the optimal thickness is available, corresponding to the highest heat transfer enhancement. The effect of thickness on the boiling heat transfer is related to the pore density, and the optimal thickness decreases with the increase of PPI value. In this experiment, the foamed metal specimens with pore density of 20, 40, 80 PPI correspond to the optimal thickness of 8, 6, 3 mm, respectively.

It can be concluded that, the foamed metal welded surface can significantly enhance the pool boiling heat transfer and the enhancing effect is related to pore density, thickness and other intrinsic parameter as well as the actual operating condition (such as heat flux density applied).

## 4 Conclusions

Pool boiling heat transfer experiments are performed on copper foam welded surfaces with various parameters in de-ionized water to investigate the enhancement of heat transfer performance. The enhancement mechanism is also discussed. Main conclusions can be drawn as follows.

Copper foam welded surfaces can significantly enhance the pool boiling heat transfer performance compared with smooth plain surface. The boiling incipience temperature can be reduced by 7—9 K, and the heat transfer coefficient can reach 5.9 W/(cm²·K), which is maximally about two times of that of smooth plain surface. These excellent performances are attributed to numerous nucleation sites, extended surface areas, and enhanced turbulent effect caused by irregular skeleton of metal foam during bubble release.

The foam PPI has two opposite effects on the pool boiling heat transfer. Higher PPI with smaller pore diameter provides more potential nucleation sites, larger heat transfer area and capillary-assisted force sucking working fluid, which can enhance pool boiling heat transfer. But smaller pore diameter leads to greater resistance to bubble release, which can deteriorate heat transfer. Especially, the bubble release resistance plays a dominant role at high heat flux density regime.

The foam thickness similarly influences the pool boiling heat transfer from two opposite sides. Larger thickness provides more potential nucleation sites and larger heat transfer area, but generates

larger resistance to bubble release due to longer transport distance inside the foam structure. The optimal thickness decreases from 8 mm to 3 mm with increase of PPI value from 20 to 80.

## References


[1] TARIQ H A, ISRAR A, KHAN Y I, et al. Numerical and experimental study of cellular structures as a heat dissipation media[J]. Heat and Mass Transfer, 2019, 55(2): 501-511.

[2] PARK K J, JUNG D, SHIM S E. Nucleate boiling heat transfer in aqueous solutions with carbon nanotubes up to critical heat fluxes[J]. International Journal of Multiphase Flow, 2009, 35(6): 525-532.

[3] KUANG Y C, CHONG L D, TSUNG C. Pool boiling heat transfer on artificial micro-cavity surfaces in dielectric fluid FC-72[J]. Journal of Micromechanics and Microengineering, 2006, 16(10): 2092-2099.

[4] NIU G, LI J. Visualization study of pool boiling on polished and porous coated surfaces for deionized water and $Al_2O_3$-water nano-fluids[C]//Proceedings of ASME International Mechanical Engineering Congress and Exposition. [S.l.]: American Society of Mechanical Engineers, 2013.

[5] ALAM M S, PRASAD L, GUPTA S C, et al. Enhanced boiling of saturated water on copper coated heating tubes[J]. Chemical Engineering and Processing: Process Intensification, 2008, 47(1): 159-167.

[6] LI C, WANG Z, WANG P I, et al. Nanostructured copper interfaces for enhanced boiling[J]. Small, 2008, 4(8): 1084-1088.

[7] MORI S, OKUYAMA K. Enhancement of the critical heat flux density in saturated pool boiling using honeycomb porous media[J]. International Journal of Multiphase Flow, 2009, 35(10): 946-951.

[8] MORI S, AZNAM S M, OKUYAMA K. Enhancement of the critical heat flux density in saturated pool boiling of water by nanoparticle-coating and a honeycomb porous plate[J]. International Journal of Heat and Mass Transfer, 2015, 80: 1-6.

[9] LI X, BOHN P. Metal-assisted chemical etching in $HF/H_2O_2$ produces porous silicon[J]. Applied Physics Letters, 2000, 77(16): 2572-2574.

[10] KOUSALYA A S, WEIBEL J A, GARIMELLA S V, et al. Metal functionalization of carbon nanotubes for enhanced sintered powder wicks[J]. International Journal of Heat and Mass Transfer, 2013, 59: 372-383.

[11] UJEREH S, FISHER T, MUDAWAR I. Effects of carbon nanotube arrays on nucleate pool boiling[J]. International Journal of Heat and Mass Transfer, 2007, 50(19): 4023-4038.

[12] XU P, LI Q, XUAN Y. Enhanced boiling heat transfer on composite porous surface[J]. International Journal of Heat and Mass Transfer, 2015, 80: 107-114.

[13] EL-GENK M S, ALI A F. Enhanced nucleate boiling on copper micro-porous surfaces[J]. International Journal of Multiphase Flow, 2010, 36(10): 780-792.

[14] LI S, FURBERG R, TOPRAK M S, et al. Nature-inspired boiling enhancement by novel nanostructured macroporous surfaces[J]. Advanced Functional Materials, 2008, 18(15): 2215-2220.

[15] FURBERG R, PALM B. Boiling heat transfer on a dendritic and micro-porous surface in R134a and FC-72[J]. Applied Thermal Engineering, 2011, 31(16): 3595-3603.

[16] XU J, YANG M J, XU J L, et al. Vertically oriented $TiO_2$ nanotube arrays with different anodization times for enhanced boiling heat transfer[J]. Science China Technological Sciences, 2012, 55(8): 2184-2190.

[17] ZHANG B J, KIM K J, YOON H. Enhanced heat transfer performance of alumina sponge-like nano-porous structures through surface wettability control in nucleate pool boiling[J]. International Journal of Heat and Mass Transfer, 2012, 55(25): 7487-7498.

[18] YANG X, YU J, GUO Z, et al. Role of porous metal foam on the heat transfer enhancement for a thermal energy storage tube[J]. Applied Energy, 2019, 239: 142-156.

[19] LAFDI K, ALMAJALI M, HUZAYYIN O. Thermal properties of copper-coated carbon foams[J]. Carbon, 2009, 47(11): 2620-2626.

[20] MINKOWYCZ W, HAJI-SHEIKH A, VAFAI K. On departure from local thermal equilibrium in porous media due to a rapidly changing heat source: The sparrow number[J]. International Journal of Heat and Mass Transfer, 1999, 42(18): 3373-3385.

[21] JIN L, LEONG K, PRANOTO I. Saturated pool boiling heat transfer from highly conductive graphite foams[J]. Applied Thermal Engineering, 2011, 31(14): 2685-2693.

[22] XU J, JI X, ZHANG W, et al. Pool boiling heat transfer of ultra-light copper foam with open cells[J]. International Journal of Multiphase Flow, 2008. 34(11): 1008-1022.


**Acknowledgements** This work was supported by the National Natural Science Foundation of China (No.52075249), and the Foundation of Jiangsu Key Laboratory of Bionic Functional Materials(No. NJ2020026).

**Authors** Mr. **HU Zhuoyang** is a postgraduate student

in College of Mechanical and Electrical Engineering, Nanjing University of Aeronautics and Astronautics. His research interest is focused on bionic surface/interface technology.

Dr. **JI Keju** is an associate professor at College of Mechanical and Electrical Engineering, Nanjing University of Aeronautics and Astronautics. His research interests include micro/nano manufacturing technology, bionic adhesive materials, and industrialization of bionic interface materials.

**Author contributions** Dr. **JI Keju** carried out the conception and designed the experiments of the study. Mr. **HU Zhuoyang** carried out experimental research, and wrote the draft of manuscript. Mr. **CUI Enhua** helped build the experimental setup and analyzed the heat transfer performance. Mr. **KHAN Muhammad Niaz** carried out the bubble formation analysis, and wrote partial draft of manuscript. Mr. **ZHANG Qian** carried out some theoretical research about the pool boiling experiment. Mr. **CHEN Xuefeng** carried out the editing of some figures and provided some experimental equipment. All authors commented on the manuscript draft and approved the submission.

**Competing interests** The authors declare no competing interests.

(Production Editor: WANG Jing)

# 开孔泡沫铜在池沸腾中的强化传热性能研究

胡卓扬, 崔恩华, KHAN Muhammad Niaz, 张迁, 陈雪锋, 姬科举

(南京航空航天大学机电学院,南京 210016,中国)

**摘要:** 多孔结构在池沸腾过程中的强化传热性能研究对热管理技术具有重要意义。本文在以去离子水作为介质的可视化热管装置中开展了泡沫铜池沸腾传热实验研究,分析了不同孔密度泡沫铜基本参数对强化传热的影响。观测研究开孔泡沫铜内部及表面沸腾现象,特别是气泡在泡沫铜三维骨架空间中的成核与逸出方式,对比考察了泡沫铜多孔结构孔密度与结构厚度对池沸腾传热性能的影响规律。结果表明,泡沫铜的孔密度和厚度对池沸腾传热特性具有较大影响,较高孔密度的泡沫铜因其多孔结构带来的大表面积与高孔隙率特征,在流固耦合界面可以形成大量的成核点,可以显著提高池沸腾的传热性能,使沸腾起始温度降低7~9 ℃,与光滑平面相比,传热系数达到2倍,展示出多孔金属的结构与表面优势。

**关键词:** 泡沫铜;多孔表面;强化传热;池沸腾